Metrol. Meas. Syst., Vol. XXII (2015), No. 4, pp. 479–490.

PAN POLSKA AKADEMIA NAUK

METROLOGY AND MEASUREMENT SYSTEMS

Index 330930, ISSN 0860-8229
www.metrology.pg.gda.pl

M&MS

SURFACE TOPOLOGY RECONSTRUCTION FROM THE WHITE LIGHT INTERFEROGRAM BY MEANS OF PRONY ANALYSIS

Anna Khoma[1)], Jarosław Zygarlicki[2)]

1) Lviv Politechnical National University, Faculty of Computer Technologies, Automation and Metrology, St. Bandery 12, 79-013 Lviv, Ukraine (avkhoma@gmail.com)

2) Opole University of Technology, Faculty of Electrical Engineering, Automatic Control and Informatics, Prószkowska 76, 45-758 Opole, Poland (✉ j.zygarlicki@po.opole.pl, +48 77 449 8074)

Abstract

The paper presents a new method of surface topology reconstruction from a white light interferogram. The method is based on interferogram modelling by complex exponents (Prony method). The compatibility of white light interferogram and Prony models has already been proven. Effectiveness of the method was tested by modelling and examining reconstruction of tilted and spherical surfaces, and by estimating the reconstruction accuracy.

Keywords: white light interferometry, surface reconstruction, Prony approximation method.

© 2015 Polish Academy of Sciences. All rights reserved

1. Introduction

In many fields of science and technology appears a need of measuring surface parameters, such as the surface profile, roughness, *etc*. In recent years, *white light interferometry* (WLI) is of significant interest for the reconstruction of surface profile. The advantages of this technology include its non-intrusiveness, high resolution, and the possibility to examine step-like surfaces [1–6].

In contrast to conventional monochrome light interferometry, analysis of a white light interferogram for the surface topology reconstruction is more complicated. This is caused by an envelope effect influencing the signal intensity. Currently, a number of reconstruction methods have been developed, for example the method of envelope detection or determination of maximum intensity in the spatial domain, the phase-shifting method, or the Fourier transform in the frequency domain [7–11]. However, such methods are not effective in many cases, *e.g.* for surfaces with non-linear shapes [12, 13].

Thus, it is still an open question to develop new effective methods for the surface reconstruction, based on an interferometer image obtained by means of WLI. This paper describes a new interferometry method for the surface topology reconstruction, based on modelling of an interferogram with complex exponents, known as the Prony method. The study results indicate efficiency of the method and enable to determine its restrictions.

2. Physical principles of white light interferometry and mathematical model of interferogram

An interference occurs as a result of superposition of two or more coherent light waves. In effect, the total wave is amplified or attenuated (the light and dark bands on the interferogram). Interferometers are optical instruments using the interference for measurement of geometrical

- 10.1515/mms-2015-0049

Downloaded from De Gruyter Online at 09/23/2016 10:37:18AM
via Politechnika Swietokrzyska - Kielce University of Technology

Article history: received on Jul. 01, 2015; accepted on Sep. 07, 2015; available online on Dec. 07, 2015; DOI: 10.1515/mms-2015-0049.

properties, including studies of the surface topology. Modern white light interferometers, such as Talysurf CCI 6000, provide measurement along the vertical axis with a resolution below 1 Å.

The principle of operation of an interferometer is explained in Fig. 1.

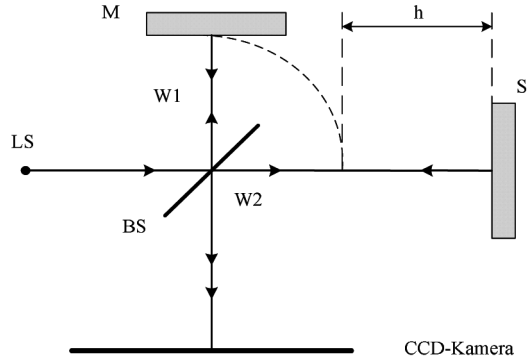

Fig. 1. A general design of interferometer.

The LS (*light source*) illuminates the BS (*beam splitter*), which leads to formation of two light beams: W1 and W2. The beams reflected from the reference mirror M and the examined surface S in BS are superposed and form an image of interference bands recorded by a CCD camera (Fig. 2). The maximum light intensity (light areas) is observed when the difference of optical paths W1 and W2 is equal to or is a multiple of the wavelength, while the inversely dark areas correspond to points where phases of waves W1 and W2 are opposite.

Figure 2 presents a fundamental difference between the images of interferograms of monochromatic light (Fig. 2b) and white light (Fig. 2c), obtained for a tilted step-like surface (Fig. 2a).

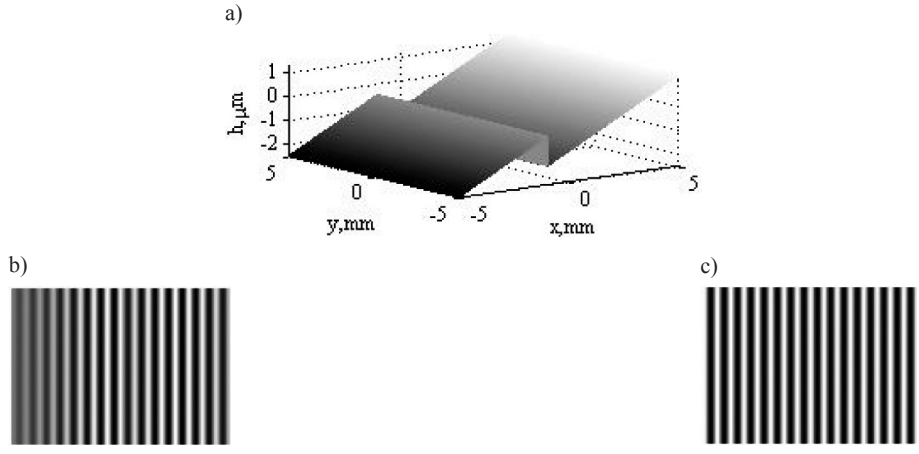

Fig. 2. a) A tilted step-like surface; b) interferograms for monochromatic light; c) white light.

The low white light correlation level causes decay of intensity of bands on image edges (Fig. 2c). Such a distinctive feature of WLI is on the one hand its advantage that enables clear reconstruction of complex step-like surfaces (in contrast to coherent monochromatic interferometry), but, on the other hand, due to the decline of band intensity, makes analysis of the interferogram more difficult [1].

- 10.1515/mms-2015-0049
Downloaded from De Gruyter Online at 09/23/2016 10:37:18AM
via Politechnika Swietokrzyska - Kielce University of Technology

The basis for the surface topology reconstruction is a mathematical model of a white light interferogram. The graph in Fig. 2b presenting the change in light intensity along the horizontal interferogram can be described with the following expression [12]:

$$I(T) = I_0 + E(T) \cdot C(T), \tag{1a}$$

$$E(T) = I_M \cdot \exp-\left(\alpha^2 \cdot T^2\right) = I_M \cdot \exp-\left(\left(\frac{2 \cdot \Delta\lambda}{\lambda_0^2}\right)^2 \cdot T^2\right), \tag{1b}$$

$$C(T) = \cos\left(\beta \cdot T\right) = \cos\left(\frac{4 \cdot \pi}{\lambda_0} \cdot T\right), \tag{1c}$$

where: I_0 and I_M – the constant component and amplitude of light intensity envelope; T – the optical difference of paths; $\alpha = \frac{2 \cdot \Delta\lambda}{\lambda_0^2}$ and $\beta = \frac{4 \cdot \pi}{\lambda_0}$ – the parameters characterising the light source; λ_0 and $\Delta\lambda$ – the middle wavelength and the width of spectral density of the white light source.

Equation (1) are a one-dimensional (1D) mathematical model of interferogram, combining the optical difference T of paths of beams reflected from the examined and reference surfaces with the pixel intensity I in each point c (column) of a selected line r (row) of the interferogram. The interferometric image (2D) is a set of such individual lines, *i.e.* the matrix of dimension $R*C$. Apart from the constant component of light intensity $I_{0,}$ the model contains two more elements: the envelope $E(T)$ in a shape of the Gaussian function and the carrier $C(T)$ in a form of the cosine function.

As shown by the (1), the desired informatic parameter T is at the same time an argument of both the envelope and the carrier. Since the measurement of such physical properties like the phase is relatively easier (in comparison to that of the intensity), the majority of reconstruction methods prefer the exact measurement of the informatic parameter T from the carrier $C(T)$. The problem of the surface profile reconstruction is thus reduced to the measurement and accumulation of the instantaneous value of frequency f_n of the interferogram carrier (1c), and the height of any point n on the surface can be obtained after re-scaling:

$$f_n = \frac{4 \cdot \pi}{\lambda_0} \cdot T_n. \tag{2}$$

Equation (1) is non-linear and non-algebraic; hence, it has no analytical solution. The simplest method to obtain the desired value T is to determine the complete phase $\Phi(T)$ of the interferogram carrier. However, it requires simultaneous minimisation of the envelope effect on the accuracy of results.

So far, a number of methods have been developed that guarantee invariability of results regarding the envelope decay, *e.g.* on the basis of the Fourier or Hilbert transform. However, the reconstruction of non-linear surfaces with these methods is imprecise [13, 14]. Therefore, new methods of reconstruction are being sought for that would enable engineering accuracy and would be computationally efficient. Below we present the results of the development of a new approach to white light interferometry for the surface reconstruction, based on the Prony method.

- 10.1515/mms-2015-0049
Downloaded from De Gruyter Online at 09/23/2016 10:37:18AM
via Politechnika Swietokrzyska - Kielce University of Technology

3. Theoretical basics of Prony method

Despite the fact that the Prony method was developed in the late 18th century [15], it currently has a number of variations [16–19]. It is a powerful tool for modelling sampled experimental data $\mathbf{s} = \{s_1, s_2,...,s_N\}$, using the sum p of complex exponents:

$$\hat{s}_n = \sum_{k=1}^{p} a_k \cdot e^{(\sigma_k + j2\pi f_k)\cdot(n-1)\cdot\Delta + j\theta_k} = \sum_{k=1}^{p} h_k \cdot z_k^{n-1} \quad , \tag{3}$$

where: $\tilde{s}_n$ – the signal estimate; a_k and σ_k – the amplitude attenuation factor of the k-th exponent; f_k and θ_k – the frequency and initial phase of the k-th component; n – the sample number; Δ – the sampling period of interferogram.

In the Prony model (3), for convenience of analysis and simpler determination of the parameters a_k, σ_k, f_k and φ_k, the time-independent element:

$$h_k = a_k \cdot e^{j\theta k} \tag{4}$$

and the time-dependent component:

$$z_k = e^{(\sigma_k + j2\pi f_k)\cdot\Delta} \tag{5}$$

were isolated.

The model parameters a_k, σ_k, f_k and θ_k are selected in such a way, so as to obtain the mean square error of difference of analysed signal samples s_n and its estimate $\tilde{s}_n$ (2) minimised:

$$\varepsilon^2 = \sum_{n=1}^{N} (s_n - \hat{s}_n)^2 = \sum_{n=1}^{N} (s_n - \sum_{k=1}^{p} h_k \cdot z_k^{n-1})^2. \tag{6}$$

In the original Prony method for modelling signals with real values of samples, the order p of the model enables to determine $p/2$ parameters of complex exponents grouped in coupled pairs. This requires $N = 2p$ samples.

Thus, the (3) can be written in a matrix form, based on the values (4) and (5):

$$\begin{pmatrix} z_1^0 & z_2^0 & \cdots & z_p^0 \\ z_1^1 & z_2^1 & \cdots & z_p^1 \\ \vdots & \vdots & \cdots & \vdots \\ z_1^{p-1} & z_2^{p-1} & \cdots & z_p^{p-1} \end{pmatrix} \times \begin{pmatrix} h_1 \\ h_2 \\ \vdots \\ h_p \end{pmatrix} = \begin{pmatrix} s_1 \\ s_2 \\ \vdots \\ s_p \end{pmatrix}. \tag{7}$$

From the (7) two unknown values shall be determined, *i.e.* the matrix $\boldsymbol{z}$ and the vector $\mathbf{h}$, and, in effect, the model parameters a, f, σ and θ.

One of the methods for determining the Prony model is derived from the theory of Digital Signal Processing and consists of the following steps [16, 20, 21]:

1. Creating a Toeplitz matrix from the samples of modelled signal:

$$\begin{pmatrix} s_p & s_{p-1} & \cdots & s_1 \\ s_{p+1} & s_p & \cdots & s_2 \\ \vdots & \vdots & \cdots & \vdots \\ s_{2p-1} & s_{2p-2} & \cdots & s_p \end{pmatrix} \times \begin{pmatrix} A_1 \\ A_2 \\ \vdots \\ A_p \end{pmatrix} = \begin{pmatrix} s_{p+1} \\ s_{p+2} \\ \vdots \\ s_{2p} \end{pmatrix}. \tag{8}$$

2. Solving the matrix equation in order to determine vector elements $\{A_i\}$ that are the coefficients of characteristic polynomial:

$$P(z) = A_0 \cdot z^p + A_1 \cdot z^{p-1} + \ldots + A_{p-1} \cdot z + A_p = \sum_{i=0}^{p} A_i \cdot z^{p-i}, \tag{9}$$

where: $A_0 = 1$.

- 10.1515/mms-2015-0049
Downloaded from De Gruyter Online at 09/23/2016 10:37:18AM
via Politechnika Swietokrzyska - Kielce University of Technology

3. Determining the unknown complex root z_k from the characteristic (9):

$$P(z)=\prod_{k=1}^{p}(z-z_k)=(z-z_1)\cdot(z-z_2)\cdot\ldots\cdot(z-z_p)=0.$$

4. Calculating the time-dependent model parameters (frequency f_k, attenuation σ_k) from the complex roots:

$$f_k=\frac{1}{2\pi\Delta}arctg\frac{\mathrm{Im}(z_k)}{\mathrm{Re}(z_k)}, \tag{10}$$

$$\sigma_k=\frac{\ln|z_k|}{\Delta}. \tag{11}$$

5. Creating a Vandermonde matrix from the roots z_k:

$$V=\begin{pmatrix}1 & 1 & \ldots & 1\\ z_1 & z_2 & \cdots & z_p\\ \vdots & \vdots & \ldots & \vdots\\ z_1^{N-1} & z_2^{N-1} & \cdots & z_p^{N-1}\end{pmatrix}. \tag{12}$$

6. Solving the matrix equation in order to determine the model parameters (amplitude a_k and initial phases θ_k of cosine curves) that are time-independent:

$$a_k=|h_k|, \tag{13}$$

$$\theta_k=arctg\frac{\mathrm{Im}(h_k)}{\mathrm{Re}(h_k)}. \tag{14}$$

Based on the parameters determined in such a way, the signal intensity can be replaced with its estimates. However, in order to reconstruct the surface profile it is sufficient to determine only one model parameter – a set of instantaneous frequencies – and then calculate the full phase of the carrier. Therefore, there is no need to calculate the three remaining parameters and reconstruct the interferogram with the set of complex exponents, which decreases demand on computational power of the used surface reconstruction method.

4. Adaptation of interferogram signal to Prony model

It is impossible to directly apply the Prony method to solve (1) to obtain the value of T, as the interferogram model (1) cannot be represented by the set of complex exponents. In order to check suitability of the Prony method, we will test the possibility of replacing the envelope in the interferogram function (Gaussian function) by co-sinusoidal windows.

A general form of the co-sinusoidal window family can be described by the following expression [22]:

$$W(n)=w_0+\sum_{i=1}^{L}\left[w_i\cdot\cos\left(2\pi\frac{n}{N-1}\right)\right], \tag{15}$$

where: N – the number of signal samples; w_i – the constant coefficients determined by the type of the window; L – the window order.

Increasing the order L decreases the approximation error for the Gaussian curve (see Table 1).

- 10.1515/mms-2015-0049
Downloaded from De Gruyter Online at 09/23/2016 10:37:18AM
via Politechnika Swietokrzyska - Kielce University of Technology

Table 1. Dependence of the mean-square error of envelope approximation for a white light interferogram on the co-sinusoidal window order.

Surface type	Error of approximation (%) with window type			
	Hann (I)	Blackman (II)	Nuttall (III)	Blackman-Harris (III)
Linear (T = n)	5.6	2.5	0.38	0.28
Non-linear (T =n^2)	4.9	2.3	0.36	0.25

The satisfactory approximation results are obtained for the third-order window functions. Thus, the Gaussian envelope can be replaced with a Blackman-Harris window with the coefficients: $w_0 = 0.35875$, $w_1 = -0.48829$, $w_2 = 0.14128$, $w_3 = -0.01168$, and the mean square error below 0.3%:

$$E(T) = e^{-\alpha T^2} \approx \approx w_0 + w_1 \cdot \cos(\alpha \cdot T) + w_2 \cdot \cos(2\alpha \cdot T) + w_3 \cdot \cos(3\alpha \cdot T). \tag{16}$$

Finally, taking into account (16), the interferogram signal can be represented by the sum of cosines:

$$I(T) = I_M \cdot \exp^{-\alpha \cdot T^2} \cdot \cos(\beta \cdot T) = I_M \cdot w_0 \cdot \cos \beta T + I_M \cdot w_1 \cdot [\cos(\beta - \alpha)T + \cos(\beta + \alpha)T] + + I_M \cdot w_2 \cdot [\cos(\beta - 2\alpha) \cdot T + \cos(\beta + 2\alpha) \cdot T] + I_M \cdot w_3 \cdot [\cos(\beta - 3\alpha) \cdot T + \cos(\beta + 3\alpha) \cdot T], \tag{17}$$

where: α and β – the constant coefficients defined by the source light parameters (1b) and (1c).

5. Implementation of Prony method in the field of white light interferometry

Analysis of the fitted interferogram signal model (17) indicates that the dominant element for sections of envelope decay (outside the central section of the window) is the interferogram carrier. Therefore, the second-order Prony model is sufficient to determine its full phase. In order to create a Toeplitz matrix for the second-order model, the following values are needed: the current sample value n and three future samples of the interferogram signal:

$$\begin{pmatrix} I_{n+1} & I_n \\ I_{n+2} & I_{n+1} \end{pmatrix} \times \begin{pmatrix} A_1 \\ A_2 \end{pmatrix} = \begin{pmatrix} I_{n+2} \\ I_{n+3} \end{pmatrix}. \tag{18}$$

The Toeplitz matrix enables to determine the signal parameters at the moment n, and since n is defined in space from 1 to N, the signal synthesis can be accomplished in N-3 points.

For the Prony model defined in such a way (based on four signal samples), the interferogram signal parameters (including the instantaneous frequency) can be seen as constant values.

After solving the system of 2nd order equations, the coefficients A_1 and A_2 will be determined:

$$A_{1n} = \frac{I_n \cdot I_{n+3} - I_{n+1} \cdot I_{n+2}}{I_{n+1}^2 - I_n \cdot I_{n+2}}, \qquad A_{2n} = \frac{I_{n+2}^2 - I_{n+1} \cdot I_{n+3}}{I_{n+1}^2 - I_n \cdot I_{n+2}}, \tag{19}$$

of the characteristic equation: $z^2 + A_{1n} \cdot z + A_{2n} = (z - z_1) \cdot (z - z_2) = 0.$

- 10.1515/mms-2015-0049
Downloaded from De Gruyter Online at 09/23/2016 10:37:18AM
via Politechnika Swietokrzyska - Kielce University of Technology

The roots of the equation are determined using the formula:

$$z_{n1,n2} = -\frac{A_{1n}}{2} \pm \sqrt{\left(\frac{A_{1n}}{2}\right)^2 - A_{2n}} \,. \tag{20}$$

The instantaneous frequencies are calculated based on the (10): $f_n = \frac{1}{2\pi\Delta} arctg \frac{\mathrm{Im}(z_n)}{\mathrm{Re}(z_n)}$, and it is possible to calculate the optical path difference in the individual surface points along the analysed single (1D) line of interferogram:

$$T_n = \frac{\lambda_0}{2\pi}\Phi(T) = \frac{\lambda_0}{2\pi} cumsum\left[2\pi\Delta f_n\right], \tag{21}$$

where: the *cumsum* function means the cumulative sum.

The geometric height of surface points is obtained on the basis of the relation:

$$h_n = \frac{T_n}{\nu}, \tag{22}$$

where: v – the refractive index of the surrounding medium.

The reconstruction (2D) of the entire surface requires application of the Prony method for each line of the interferogram. Examining the properties and accuracy of the Prony method in the problem of surface topology reconstruction based on a white light interferogram was carried out on the examples of a linear tilted surface and a non-linear spherical surface.

6. Reconstruction of tilted surface and study of errors for various angles of inclination

The analysis of the Prony method accuracy was performed for simulated surfaces. For simulations a white light source with parameters: $\lambda_0 = 620$ nm and $\Delta\lambda = 51.6$ nm was selected; thus, the factors α and β equalled to: $\alpha = 0.269 \cdot 10^6$ m^{-1} and $\beta = 20.3\ 10^6$ m^{-1}, respectively.

Figure 3a presents a flat 10 × 10 mm surface with inclination of:

$$\mathrm{tg}\ \varphi = (T_{max} - T_{min})/X = 5\ \mu\mathrm{m}/10\ \mathrm{mm} = 5*10^{-4},$$

(T_{max} i T_{min} – the maximum and minimum values of optical path difference, X – the range of CCD camera along the horizontal axis), while Fig. 3b shows the image of its interferogram for the above source light parameters. For low values of the angle, the following relation holds: tg $\varphi \approx \varphi = 500$ μrad.

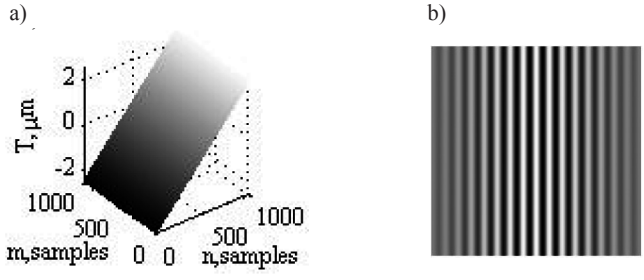

Fig. 3. a) A tilted surface; b) its corresponding interferogram.

In the modelling, application of a CCD camera with 1000 × 1000 px was assumed; therefore, the sampling period in space (lateral resolution) is 10 μm. Fig. 4 presents the curve of intensity function, *i.e.* a single interferogram line.

- 10.1515/mms-2015-0049
Downloaded from De Gruyter Online at 09/23/2016 10:37:18AM
via Politechnika Swietokrzyska - Kielce University of Technology

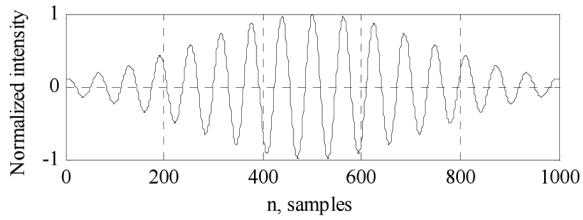

Fig. 4. The representation of 1D line of WLI.

After application of the Prony method for the intensity signal, the surface profile was reconstructed. The accuracy of reconstruction evaluated by the total error can be calculated for each sample of the interferogram:

$$\gamma(n) = \frac{T_R(n) - T(n)}{T_{\max} - T_{\min}} \cdot 100\%, \tag{23}$$

and the mean square error:

$$\sigma = \frac{\sqrt{\sum_{n=1}^{N} \left[T_R(n) - T(n)\right]^2}}{N \cdot \left[T_{\max} - T_{\min}\right]} \cdot 100\%, \tag{24}$$

where: $T(n)$ – the optical path difference for the n-th sample of simulated surface; and $T_R(n)$ – the value of optical path difference for the n-th sample of the interferogram, estimated by the Prony method.

Dependence of the total reconstruction error on the number of samples is presented in Fig. 5.

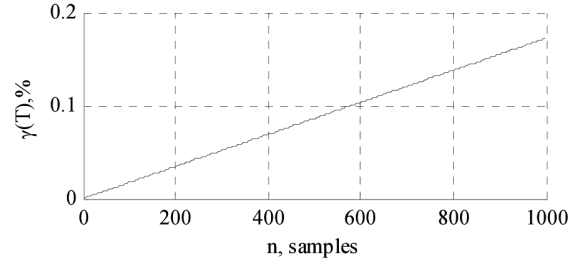

Fig. 5. The reconstruction error graph for a tilted surface profile.

As can be seen, the reconstruction error increases with the number of samples, but it does not exceed 0.2% for the inclination angle φ = 500 μrad of a linear surface.

Table 2 summarises the reconstruction errors (the maximum and mean square errors) for a tilted surface profile for various angles of inclination.

Table 2. Dependence of the mean square and maximum errors for the reconstruction of a tilted surface profile on the angle of its inclination.

φ, μrad	1000	500	200	100	50
σ, %	0.099	0.099	0.099	0.1	0.097
γ_{max}, %	0.17	0.17	0.17	0.18	0.17

The studies presented a controversial impact of the inclination degree on the reconstruction error using the Prony method (φ > 100 μrad). We observe a negative effect of the envelope

- 10.1515/mms-2015-0049
Downloaded from De Gruyter Online at 09/23/2016 10:37:18AM
via Politechnika Swietokrzyska - Kielce University of Technology

(decline in the intensity at the beginning and end of the image) on the accuracy of determination of instantaneous frequencies. However, for angles below 0.05 μrad the reconstruction error drastically increased, due to improper conditioning of the Toeplitz matrix.

7. Reconstruction of spherical surface and studies of errors for various curvatures

The issue of application of the Prony method for the spherical surface reconstruction was studied with the assumptions described in the previous section. Fig. 6a presents a spherical surface with the height of the cap equal to 2.5 μm. The image of its interferogram is shown in Fig. 6b.

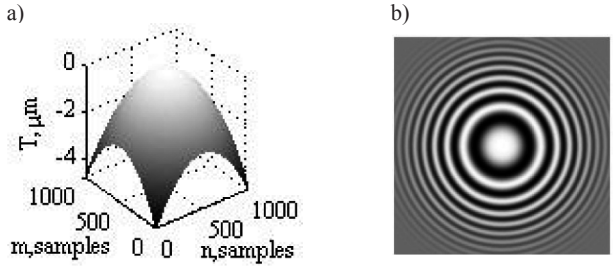

Fig. 6. a) A spherical surface; b) its corresponding interferogram.

The interferogram intensity signal for a spherical surface (Fig. 6) along the central line is presented in Fig. 7. In contrast to the intensity signal for a tilted surface (Fig. 4), the signal presented in Fig. 7 contains a visible instability of frequency. This fact is confirmed by Fig. 8 which presents changes of the frequency along the interferogram line.

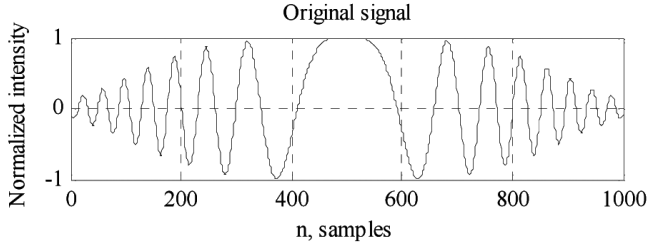

Fig. 7. The representation of 1D line of WLI.

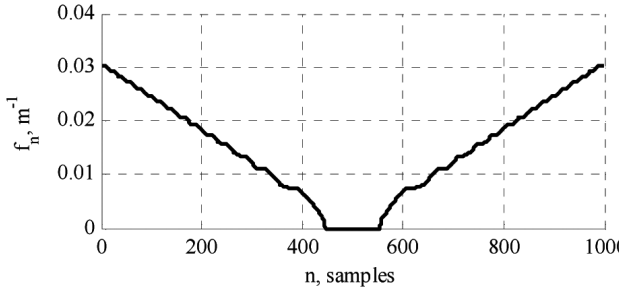

Fig. 8. Dependence of the interferogram instantaneous frequency on the number of samples.

- 10.1515/mms-2015-0049
Downloaded from De Gruyter Online at 09/23/2016 10:37:18AM
via Politechnika Swietokrzyska - Kielce University of Technology

Figure 9a presents the results of spherical surface profile reconstruction by means of the Prony method (for a better resolution of the graph, only the central fragment is presented), whereas Fig. 9b presents the reconstruction error graph. In the centre, an increase of the reconstruction error is clearly visible. This is the result of the signal mismatching the second-order Prony model. The more detailed analysis found positive values of the discriminant of characteristic equation in the range from 444 to 552, and thus no imaginary values of roots z_k, which gives zero instantaneous frequencies in these points. This requires an increasing order of the Prony model, which, however, will be accompanied with the increase of its computational complexity.

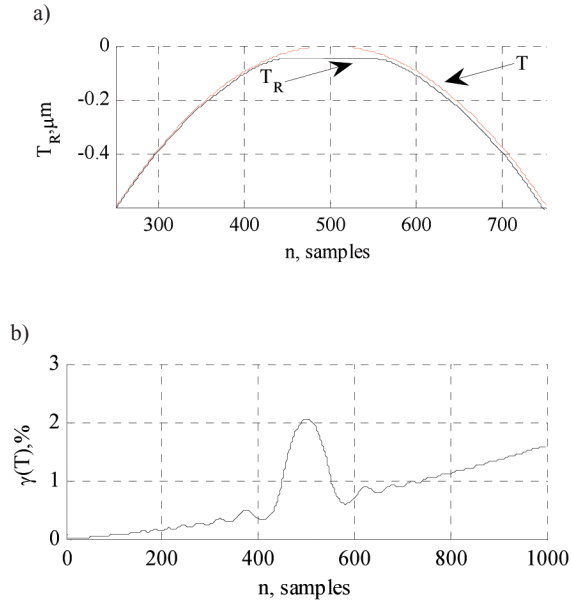

Fig. 9. The results of spherical surface reconstruction: a) the shape of the profile of the simulated surface (curve T) and the reconstructed surface (curve T_R); b) the reconstruction error graph.

Table 3 summarises the reconstruction errors (the maximum and mean square errors) for the spherical surface profile for various degrees of curvature estimated by the height of convexity.

Table 3. Dependence of the mean square and maximum errors for the reconstruction of a spherical surface profile on the degree of its curvature.

T_{max}, µm	2.5	1	0.5	0.2	0.1
σ, %	0.95	1.6	3.0	8.8	19.4
γ_{max}, %	2.0	4.1	7.6	18.3	34.6

Decreasing the height of convexity leads to relative widening of the middle part of intensity signal, where the 2nd order Prony method becomes unstable (the discriminant of characteristic equation has positive values), and hence the height of the reconstruction error for individual points of the examined spherical surface increases.

- 10.1515/mms-2015-0049
Downloaded from De Gruyter Online at 09/23/2016 10:37:18AM
via Politechnika Swietokrzyska - Kielce University of Technology

8. Conclusions

The article presents a mathematical model for the signal intensity of a white light interferogram and describes the problem of surface topology reconstruction. It also shortly presents the theoretical background of the Prony method for modelling of digital signals with a linear set of complex exponents.

It has been confirmed that it is possible to reduce canonical model of WLI (1) to a Prony model (3) via approximation of the interferogram envelope of Gaussian shape using a co-sinusoidal Blackman-Harris window function. The possibility of using the 2nd order Prony model for the surface topology reconstruction from a white light interferogram was justified.

The accuracy of the Prony method was tested on the example of reconstruction of tilted and spherical surfaces, showing an influence of the degree of inclination and curvature on the reconstruction accuracy.

References

[1] Wyant, J.C. (2002). White light interferometry. *Proc. SPIE 2002*, 4737, 98–107.

[2] Goodwin, E.P., Wyant, J.C. (2006). *Interferometric Optical Testing*. Washington: SPIE Press.

[3] Whitehouse, D.J. (1997). Surface metrology. *Meas. Sci. Technol.*, 8, 955–972.

[4] Świrniak, G., Głomb, G., Mroczka, J. (2014).Inverse analysis of the rainbow for the case of low-coherent incident light to determine the diameter of a glass fiber. *Applied Optics*. 53(19), 4239–4247.

[5] Świrniak, G., Glomb, G., Mroczka, J. (2014). Inverse analysis of light scattered at a small angle for characterization of a transparent dielectric fiber. *Applied Optics*. 53(30), 7103–7111.

[6] Mroczka, J., Szczuczyński, D. (2013). Improved technique of retrieving particle size distribution from angular scattering measurements. *Journal of Quantitative Spectroscopy and Radiative Transfer*. 129, 48–59.

[7] Muhamedsalih, H.M. (2013). *Investigation of wavelength scanning interferometry for embedded metrology*. Ph.D. Thesis, Univ. of Huddersfield.

[8] Magalhaes, P., Neto, P., Magalhães, C. (2010). New carré equation. *Metrol. Meas. Syst*., 17(2), 173–194.

[9] Adamczak, S., Makieła, W., Stępień, K. (2010). Investigating advantages and disadvantages of the analysis of a geometrical surface structure with the use of fourier and wavelet transform. *Metrol. Meas. Syst*., 17(2), 233–244.

[10] Borkowski, J., Mroczka, J. (2010). LIDFT method with classic data windows and zero padding in multifrequency signal analysis. *Measurement*, 43(10), 1595–1602.

[11] Borkowski, J., Mroczka, J. (2002). Metrological analysis of the LIDFT method. *IEEE Transactions on Instrumentation and Measurement*. 51(1), 67–71.

[12] Stadnyk, B., Manske, E., Khoma, A. (2014). State and prospects of computerized systems monitoring the topology of surfaces, based on white light interferomertry. *Computational Problems of Electrical Engineering*, 4(1), 75–80.

[13] Abdul-Rahman, H. (2007). *Three-dimensional fourier fringe analysis and phase unwrapping*. Ph.D. Thesis. Liverpool John Moores University.

[14] Khoma, A. (2014). Method of surface reconstruction from white light interferogram based on Hilbert transform. *Computer Science and Information Technology,* Lviv Polytechnic National University, 800, 168–175.

[15] Baron de Prony, G.R. (1795). Essai experimental et analytique: sur les lois de La dilatabilité de fluides élastique et sur celles de la force expansive de la vapeur de l'alkool, á différentes temperatures. *J. l'École Polytech*., 1(22), 24–76.

[16] Zygarlicki, J., Mroczka, J. (2012). Variable-frequency Prony method in the analysis of electrical power quality. *Metrol. Meas. Syst.*, 19(1), 39–48.

[17] Zygarlicki, J., Mroczka, J. (2014). Prony's method with reduced sampling – Numerical aspects. *Metrol. Meas. Syst.*, 21(3), 521–534.

- 10.1515/mms-2015-0049
Downloaded from De Gruyter Online at 09/23/2016 10:37:18AM
via Politechnika Swietokrzyska - Kielce University of Technology

[18] Zygarlicki, J., Mroczka, J. (2012). Prony's method used for testing harmonics and interharmonics in electrical power systems. *Metrol. Meas. Syst*., 19(4), 659–672.

[19] Zygarlicki, J., Zygarlicka, M., Mroczka, J., Latawiec, K.J. (2010). A reduced prony's method in power-quality analysis-parameters selection. *IEEE Transactions on Power Delivery,* 25(2), 979–986.

[20] Marple, S., Lawrence, Jr. (1987). *Digital Spectral Analysis*. New Jersey: Prentice Hall PTR.

[21] Lyons, R.G. (2010). *Understanding Digital Signal Processing.* Pearson Education, Inc.

[22] Ifeachor, E.C., Jervis, B.W. (2002). *Digital signal processing: a practical approach.* England: Pearson Education, 2nd ed.

- 10.1515/mms-2015-0049
Downloaded from De Gruyter Online at 09/23/2016 10:37:18AM
via Politechnika Swietokrzyska - Kielce University of Technology